*Applied Science and Engineering Progress, Vol. 20, No. 2, 2027, 8256*

Research Article

# Edge-Enabled Digital Twin for Autonomous Low-Latency Dissolved Oxygen Control for Partial Nitritation-Anammox Reactor

Micko Tomas and Zaini Zaini
Department of Electrical Engineering, Faculty of Engineering, Universitas Andalas, Padang, Indonesia

Zulkarnaini Zulkarnaini*
Department of Environment Engineering, Faculty of Engineering, Universitas Andalas, Padang, Indonesia

Ardhian Agung Yulianto
Department of Industrial Engineering, Faculty of Engineering, Universitas Andalas, Padang, Indonesia

Shahrul Ismail
Faculty of Ocean Engineering Technology and Informatics, Universiti Malaysia Terengganu, Kuala Nerus, Terengganu, Malaysia

*Corresponding author: zulkarnaini@eng.unand.ac.id DOI: 10.14416/j.asep.2026.08.002
Received: 25 March 2026; Revised: 21 May 2026; Accepted: 3 June 2026; Published online: 10 August 2026


**Abstract**
Anammox reactors are high-efficiency, energy-saving nitrogen treatment technologies, yet their process stability is highly sensitive to fluctuations in dissolved oxygen (DO). Most wastewater treatment Internet of Things systems remain limited to cloud-based monitoring without low-latency adaptive control or dynamic process representation. This study develops an edge-enabled digital twin for real-time multi-parameter monitoring and closed-loop DO control a partial nitritation-anammox reactor. The system employs an ESP32-S3 as an edge computing node for local acquisition, and monitoring of DO, ORP, pH, water temperature, TDS, room temperature, and humidity, while executing a process model dynamically synchronized with the physical reactor. Field implementation demonstrates stable operation with water temperature of 27.4 ± 0.42 °C, room temperature of 30.8 ± 0.6 °C, relative humidity of 55.2 ± 2.1%, pH of 6.21 ± 0.11, ORP of +295 ± 18 mV, and TDS of 82.6 ± 3.4 ppm. DO was maintained at a setpoint of 0.50 mg/L with ±0.03 mg/L deviation, 0.024 mg/L mean absolute error, 5.2% maximum overshoot, and 20–28 s recovery time. The edge-based control latency of 0.43 s ensures stable aeration regulation independent of cloud connectivity. The novelty lies in integrating a digital twin directly at the edge to enable autonomous DO regulation, enhancing process stability while reducing aeration energy consumption by up to 26% compared with conventional systems.

**Keywords**: Anammox reactor optimization, Closed-loop dissolved oxygen control, Cyber-physical wastewater treatment system, Edge-enabled digital twin, Energy-efficient aeration control

## 1 Introduction

Effluent of wastewater treatment plan from healthcare facilities, particularly hospitals, typically contains nitrogen concentrations instead of remain complex organic compositions and exceed of regulation limits. Whithout side stream treatment, this nitrogen content can cause eutrophication in water bodies and have serious environmental impacts. Conventional nitrogen treatment processes through nitrification–denitrification require significant aeration energy and additional external carbon sources, increasing the operational costs and energy footprint of wastewater treatment systems [1]-[4]. Therefore, the development of more efficient and sustainable nitrogen treatment technologies has become a major focus in modern wastewater treatment systems.

In the past two decades, the anaerobic ammonium oxidation (anammox) process has emerged as a promising alternative technology for nitrogen removal. This process allows the direct conversion of ammonium and nitrite to nitrogen gas under oxygen-limited conditions without the need for an external carbon source [5]-[7]. The integration of partial nitritation–Anammox (PN/A) further improves energy efficiency because only a portion of the ammonium is oxidized to nitrite before being converted to gaseous nitrogen by anammox bacteria [8]. Due to these characteristics, the PN/A process can reduce aeration requirements by up to 60% compared to conventional nitrification-denitrification systems, making it an attractive technology for sustainable wastewater treatment systems [9], [10].

However, the stability of the PN/A process is significantly affected by operational conditions, particularly dissolved oxygen (DO) concentration. Anammox bacteria are highly sensitive to high oxygen exposure, while the partial nitritation stage requires limited oxygen to produce nitrite, the primary substrate of the anammox process [11]-[14]. Therefore, controlling DO within a narrow range is key to maintaining the balance of this biological process. Uncontrolled DO fluctuations can disrupt the microbial community and reduce nitrogen removal efficiency in large-scale biological reactors [11].

The development of Internet of Things (IoT) technology has opened new opportunities for real-time monitoring of wastewater treatment systems. By utilizing a distributed sensor network, critical parameters such as DO, oxidation-reduction potential (ORP), pH, temperature, and total dissolved solids (TDS) can be continuously monitored to evaluate reactor operational conditions [15]-[19]. Cloud platforms enable remote data visualization and help operators analyze system performance. However, most IoT systems implemented in wastewater treatment still focus on monitoring and data recording functions, without adaptive process control mechanisms.

Another limitation of conventional IoT approaches is their heavy reliance on cloud-based processing. In industrial wastewater treatment systems, network communication latency and connectivity disruptions can hinder rapid decision-making in biological process control [20]-[23]. This can lead to slow system response to changing operational conditions, reducing process stability and aeration energy efficiency. Therefore, a system architecture approach capable of local data processing and low-latency decision-making is required.

In this context, the concept of edge computing is increasingly being applied to Industrial IoT systems. Edge computing enables local data processing and system control, reducing reliance on cloud infrastructure and increasing system response time [24], [25]. The integration of edge computing with real-time sensors enables faster, more stable feedback control across various industrial applications, including biological wastewater treatment systems.

DO control plays an important role in maintaining process stability and operational efficiency in various industrial and environmental systems. The proposed DO control system has potential applications in wastewater treatment systems, particularly biological nitrogen removal processes such as partial nitritation/anammox (PN/A), where precise oxygen regulation is required to maintain microbial activity and treatment performance. In addition, the system can be applied in industrial bioreactors and fermentation processes to support microbial growth and optimize product yield. Potential applications also include aquaculture systems, where stable DO levels are essential for maintaining water quality and ensuring the health of aquatic organisms. These application areas demonstrate the broader practical relevance of the proposed edge-enabled digital twin framework for real-time monitoring and control.

Furthermore, the concept of digital twins is increasingly used in modern industrial systems to represent the physical condition of a system as a real-time, synchronized digital model. Digital twins enable integrating sensor data, process modeling, and operational analysis to improve understanding of system dynamics and support continuous process optimization [26]-[28]. Although this technology has been widely applied in the smart manufacturing and infrastructure sectors, its use in biological wastewater treatment systems, particularly in large-scale PN/A reactors, remains relatively limited.

Several previous studies have examined the application of IoT in wastewater treatment system monitoring and anammox process modeling. However, most of these studies have not integrated digital twins, edge computing, and DO feedback control mechanisms into a single, integrated cyber-physical system architecture. This limitation indicates a research gap in the development of intelligent monitoring and control systems capable of adaptive and reliable operation under field conditions.

This study proposed an edge-based digital twin architecture for real-time multi-parameter monitoring and closed-loop DO control in a PN/A reactor for treating hospital wastewater. The developed system used an ESP32-S3 microcontroller as an edge computing node for local acquisition and processing of sensor data such as DO, ORP, pH, water temperature, TDS, and environmental parameters. Operational data was then synchronized with the digital twin model and visualized through the Ubidots cloud platform. The main contributions of this research include three aspects. First, the development of an edge-enabled digital twin architecture that can represent the operational conditions of the PN/A reactor in real time. Second, the implementation of an edge-based, low-latency closed-loop DO control system to maintain stable oxygen conditions in a biological reactor. Third, demonstrating the system's implementation in a PN/A reactor, improving process stability and aeration energy efficiency. Finally, the study validated the practical feasibility of integrating edge computing and digital twin technologies for autonomous, real-time control in wastewater treatment systems.

## 2 Materials and Methods

### 2.1 *System overview and experimental setup*

The proposed system was implemented on a field-scale biofilm anammox reactor with an effective working volume of 1000 L, designed to replicate realistic wastewater treatment conditions as a supplemented for existing wastewater treatment facilities. The reactor was filled with honey comb plastic media (30x30x30 cm, hole 3 cm) to improve biomass retention and facilitate the growth of slow-growing anammox bacteria, thereby improving process stability and nitrogen removal efficiency [29]-[31].

Recent studies have demonstrated that anammox systems are highly sensitive to oxygen fluctuations, requiring precise DO control to maintain process stability and efficiency [32]-[34]. To enable real-time monitoring and control, the reactor was equipped with a multi-parameter sensing system consisting of analog sensors measuring DO, ORP, pH, TDS, and water temperature. Advanced IoT-based wastewater monitoring systems have been shown to significantly enhance observability and operational performance in biological treatment processes [35]-[38]. In addition, ambient temperature and relative humidity were monitored to capture environmental influences on reactor performance. All sensor signals were interfaced with an ESP32-S3 edge computing node, which serves as the core processing unit responsible for data acquisition, pre-processing, digital twin execution, and control decision-making. Edge computing enables low-latency processing and autonomous control, overcoming limitations of cloud-based systems in real-time applications [39]-[41].

Figure 1 presents the overall system architecture of the proposed edge-enabled digital

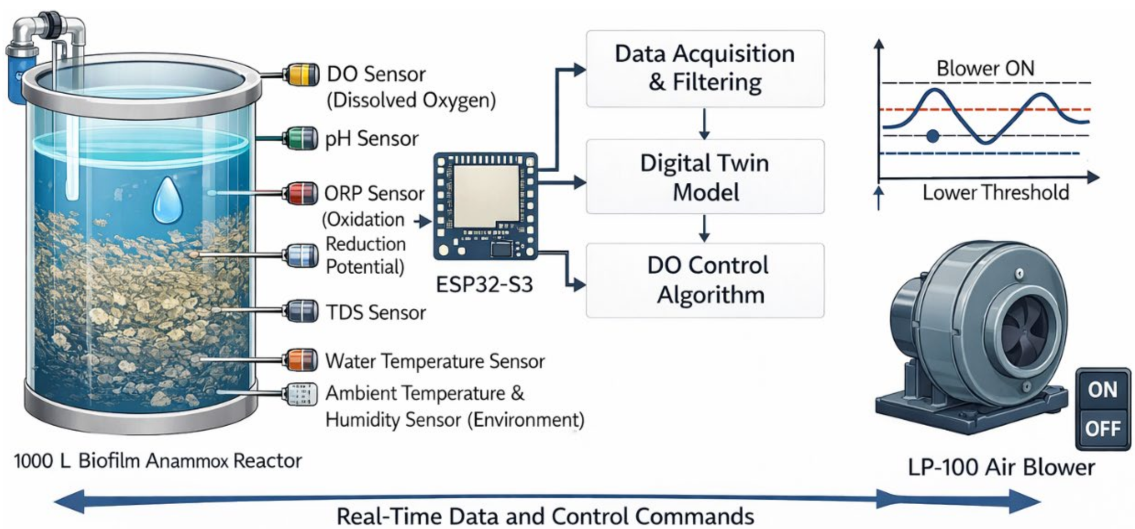


**Figure 1** : System architecture of the edge-enabled digital twin for real-time monitoring and closed-loop DO control in a field-scale Anammox reactor. The system integrates multi-parameter sensing, edge-based data acquisition and processing using ESP32-S3, digital twin modeling, and ON–OFF aeration control via an LP-100 air blower, enabling low-latency autonomous operation.

twin framework designed for real-time monitoring and closed-loop control of DO in a field-scale biofilm anammox reactor. The architecture illustrates the integration of sensing, edge computing, modeling, and actuation within a unified cyber-physical system. Recent studies highlight that integrating digital twins with edge computing enables real-time synchronization and adaptive control in complex industrial systems [42].

On the physical layer, the 1000 L biofilm anammox reactor wass equipped with multiple sensors to monitor key process and environmental variables. These include DO, pH, ORP, TDS, water temperature, and ambient temperature and humidity. Each sensor provides essential information for characterizing reactor conditions, where DO serves as the primary control variable, while the remaining parameters support process stability assessment and digital twin calibration.

The sensing data are transmitted to the ESP32-S3, which acts as the edge computing unit. At this stage, raw sensor signals are acquired and pre-processed, including filtering to reduce noise and improve signal stability. The processed data are then used by the embedded digital twin model, which represents the reactor's dynamic behavior and continuously synchronizes with real-time measurements.

Based on the digital twin output and real-time sensor feedback, a DO control algorithm is executed locally at the edge. The control strategy employs a hysteresis-based ON–OFF mechanism to maintain the DO concentration within a predefined range around the setpoint. When the DO falls below the lower threshold, the system activates the aeration unit, while exceeding the upper threshold triggers deactivation.

The actuation layer consists of an LP-100 air blower, which supplies oxygen to the reactor. The interaction between sensing, modeling, and control forms a closed-loop system that continuously regulates oxygen input based on process conditions. The bidirectional flow of information and commands, indicated by the real-time data and control pathway, highlights the system's ability to operate autonomously without relying on cloud-based computation. Figure 1 demonstrates that the proposed architecture enables low-latency, real-time decision-making by integrating a digital twin directly at the edge. This design enhances process stability, improves responsiveness, and supports energy-efficient operation in anammox-based wastewater treatment systems.

Aeration was provided by an LP-100 blower, controlled by an ON–OFF switch. This discrete actuation approach allows regulation of oxygen input based on real-time DO measurements while maintaining system simplicity and robustness. The entire system was deployed and operated continuously for 7 days under field conditions, ensuring that the collected data reflect natural variability and realistic operational constraints.

Figure 2 illustrates the complete hardware architecture of the proposed edge-enabled digital twin system designed for real-time monitoring and closed-loop control of DO in a PN/A reactor. The system integrates multiple sensing units, an edge computing platform, communication modules, and an actuator control interface, forming a fully autonomous cyber-physical system. On the sensing side, the system incorporates a set of analog and digital sensors to monitor key process and environmental variables. These include a water temperature sensor, a DO sensor, a pH sensor, an oxidation–reduction potential (ORP) sensor, a total dissolved solids (TDS/EC) sensor, and an ambient temperature and humidity sensor (DHT11). Each sensor provides critical information about the reactor condition. The DO sensor serves as the primary control variable, while pH and ORP provide insight into biochemical stability.

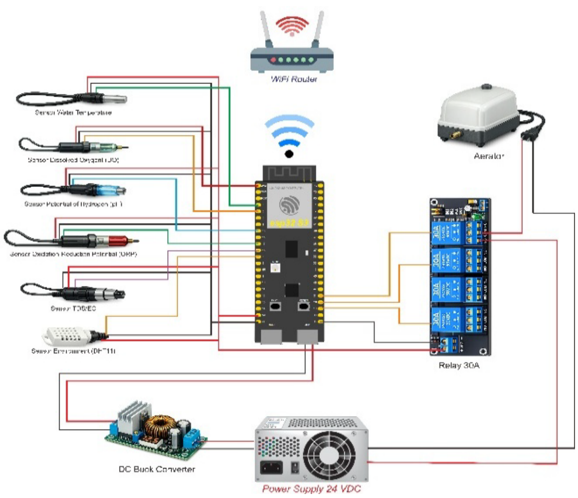


**Figure 2**: Hardware architecture of the edge-enabled digital twin system for real-time monitoring and closed-loop DO control in the Anammox reactor. The system integrates multi-parameter sensors, an ESP32-S3 edge computing unit, relay-based aeration control, and a 24 VDC power supply, enabling autonomous data acquisition, processing, and actuation.

Water temperature influences microbial kinetics, and TDS reflects dissolved matter concentration, whereas ambient conditions support system reliability assessment. All sensor signals are interfaced with the ESP32-S3 microcontroller, which functions as the edge computing node. The ESP32-S3 is responsible for real-time data acquisition, signal conditioning, filtering (e.g., moving average), and execution of the digital twin model. By processing data locally, the system minimizes latency and enables immediate control decisions without reliance on cloud infrastructure. Additionally, wireless communication via a WiFi router allows optional remote monitoring and data visualization.

The control subsystem is implemented using a relay module (30A) connected to the ESP32-S3. The relay acts as a switching interface between the low-power control signals and the high-power aeration unit (blower). Based on the control algorithm, the ESP32-S3 sends ON–OFF commands to the relay, which in turn activates or deactivates the aerator. This mechanism enables demand-based aeration, ensuring that oxygen is supplied only when required to maintain the DO setpoint.

The aeration system comprises the blower unit, which injects oxygen into the reactor. The interaction between sensor measurements and actuator control forms a closed-loop system that continuously adjusts the aeration process in real time. Power is supplied by a 24 VDC power supply, providing stable power to the entire system. A DC buck converter is used to regulate voltage levels for different components, ensuring compatibility and protecting sensitive electronics such as the ESP32-S3 and sensors. Figure 2 demonstrates how sensing, computation, communication, and actuation are tightly integrated within a single edge-based framework. This architecture enables real-time monitoring, low-latency control, and autonomous operation, which are essential for maintaining stable DO conditions and improving energy efficiency in the PN-A reactor.

### 2.2 *Edge-based data acquisition and signal preprocessing*

To ensure reliable, stable control performance, raw sensor signals were pre-processed at the edge before use for modeling and control. Given that analog sensors are prone to high-frequency noise and fluctuations, particularly in dissolved oxygen measurements, a moving average filtering technique was applied.

$$y_t = \frac{1}{N}\sum_{1=0}^{N-1} x_{t-i} \tag{1}$$

In this formulation, $y_t$ represents the filtered signal at time step $t$, $x_{t-i}$ denotes the raw sensor measurements at previous time steps, and $N$ is the window size defining the number of samples included in the averaging process. Physically, this equation computes the mean of the most recent $N$ measurements, effectively smoothing out short-term fluctuations and reducing measurement noise. The use of moving average filtering plays a critical role in enhancing control stability by preventing rapid oscillations in the control signal caused by noisy measurements. This is particularly important for ON–OFF control systems, where small fluctuations around the setpoint can otherwise lead to excessive actuator switching, commonly known as chattering.

### 2.3 *Digital twin modeling and real-time synchronization*

A custom digital twin model was developed to represent the oxygen dynamics within the PN-A reactor and was deployed directly on the edge device. Digital twin-driven wastewater systems have recently been shown to improve process prediction accuracy and operational efficiency [43], [44]. Unlike conventional digital twin implementations that operate in cloud environments, the proposed approach executes the model locally, enabling low-latency synchronization with the physical system.

The dynamic behavior of dissolved oxygen is described using a mass balance equation:

$$\frac{dDO}{dt} = k_L a(DO_{sat} - DO) - r_{O_2} \tag{2}$$

In this equation, $\frac{dDO}{dt}$ represents the rate of change of dissolved oxygen concentration over time. The term $k_L a$ denotes the oxygen transfer coefficient, which quantifies the rate at which oxygen is transferred from the gas phase into the liquid phase. $DO_{sat}$ is the saturation concentration of dissolved oxygen, while $DO$ is the current measured concentration. The term $r_{O_2}$ represents the rate of oxygen consumption by microbial activity.

Physically, the first term $k_L a(DO_{sat} - DO)$ describes oxygen transfer driven by the concentration gradient between saturation and actual $DO$ levels, while the second term $r_{O_2}$ accounts for oxygen uptake by microorganisms. This formulation captures the essential dynamics of oxygen balance within the reactor. To model biological oxygen consumption, a simplified Monod-type kinetic expression was adopted :

$$r_{O_2} = k \cdot X \cdot \frac{DO}{K_{DO} + DO} \tag{3}$$

where $k$ is the microbial kinetic rate constant, $X$ represents the active biomass concentration, and $K_{DO}$ is the half-saturation constant for dissolved oxygen. This nonlinear relationship reflects the fact that oxygen consumption increases with $DO$ concentration but eventually approaches saturation due to biological limitations.

To maintain consistency between the digital twin and the physical system, real-time parameter adaptation was implemented using an incremental update mechanism:

$$\theta(t+1) = \theta(t) + \alpha \cdot (y_{meas} - y_{\text{model}}) \tag{4}$$

Here, $\theta$ represents the model parameters, $\alpha$ is the adaptation gain, $y_{meas}$ is the measured output, and $y_{\text{model}}$ is the model-predicted output. This update rule allows the digital twin to continuously adjust its parameters based on the discrepancy between measured and simulated values, thereby improving model accuracy over time. Adaptive digital twin models improve system robustness under dynamic environmental conditions.

### 2.4 *Closed-loop DO control strategy*

A hysteresis-based ON–OFF control strategy was implemented to regulate the dissolved oxygen concentration around a predefined setpoint of 0.50 mg/L. Hysteresis-based control remains widely used in industrial aeration systems due to its robustness and low computational requirements [45]. This approach introduces a tolerance band around the setpoint to prevent excessive switching of the blower. The control thresholds are defined as:

$$DO_{low} = DO_{set} - \Delta \tag{5}$$

$$DO_{high} = DO_{set} + \Delta \tag{6}$$

where $DO_{set}$ is the target dissolved oxygen concentration and Δ represents the tolerance band. The control logic operates as follows: when the measured DO falls below $DO_{low}$, the blower is activated, and when the DO exceeds $DO_{high}$, the blower is deactivated.

From a physical perspective, this hysteresis mechanism prevents rapid toggling of the actuator when the DO concentration fluctuates near the setpoint. This improves system stability, reduces mechanical wear on the blower, and contributes to energy efficiency. Although the control strategy is relatively simple, its integration with the digital twin enhances situational awareness and enables the system to respond more effectively to process dynamics. This approach ensures a balanced trade-off between control performance and implementation complexity, making it suitable for real-time deployment.

### 2.5 *Performance evaluation metrics*

The performance of the proposed system was evaluated using multiple quantitative metrics that capture accuracy, stability, dynamic response, and energy efficiency. These metrics are widely adopted in evaluating control systems and wastewater treatment performance [46], [47].

The mean absolute error (MAE) was used to quantify control accuracy:

$$MAE = \frac{1}{n}\sum_{i=1}^{n}\left|DO_i - DO_{set}\right| \tag{7}$$

where $DO_i$ is the measured dissolved oxygen at time step $i$, $DO_{set}$ is the setpoint, and $n$ is the total number of samples. This metric represents the average absolute deviation from the desired value, with lower values indicating higher control accuracy. The maximum overshoot was calculated as:

$$M_p = \frac{DO_{\max} - DO_{set}}{DO_{set}} \times 100\% \tag{8}$$

where $DO_{\max}$ is the maximum observed DO value following a disturbance. This metric indicates how far the system exceeds the target before stabilizing, reflecting the aggressiveness of the control response.

The standard deviation was used to evaluate process stability:

$$s = \sqrt{\frac{1}{n-1}\sum_{i=1}^{n}\left(x_i - \overline{x}\right)^2} \tag{9}$$

where $x_i$ represents individual measurements and $\overline{x}$ is the mean value. This metric quantifies the dispersion of the data, with lower values indicating more stable operation.

Energy consumption was estimated based on the duty cycle of the blower:

$$E \propto \frac{T_{ON}}{T_{total}} \tag{10}$$

where $T_{ON}$ is the total duration during which the blower is active and $T_{total}$ is the total operation time. This proportional relationship allows estimation of relative energy consumption.

### 2.6 *Statistical validation*

To ensure the reliability and statistical significance of the results, both descriptive and inferential statistical analyses were performed. Statistical methods such as confidence intervals and hypothesis testing are essential for validating control system reliability in environmental monitoring systems [48]. The mean and standard deviation were calculated for all monitored variables, and the uncertainty of the estimated mean was quantified using a 95% confidence interval:

$$\overline{x} \pm t_{\alpha/2}\frac{s}{\sqrt{n}} \tag{11}$$

where $\overline{x}$ is the sample mean, $s$ is the standard deviation, $n$ is the number of samples, and $t_{\alpha/2}$ is the critical value from the Student's t-distribution.

Additionally, a one-sample t-test was conducted to evaluate whether the average DO concentration significantly differs from the target setpoint of 0.50 mg/L:

$$t = \frac{\overline{x} - \mu_0}{s / \sqrt{n}} \tag{12}$$

where $\mu_0$ represents the target DO value.

This test provides statistical evidence of the controller's ability to maintain the process near the desired operating point.

### 2.7 *Experimental protocol*

The system was operated continuously for 7 days, during which all sensor data, control actions, and model states were recorded in real time. No artificial disturbances were introduced, allowing the evaluation to reflect natural process variability and real operating conditions.

The dissolved oxygen setpoint was fixed at 0.50 mg/L, which is considered optimal for maintaining ammonium oxidizing bacteria (AOB) and anammox bacteria activity while minimizing oxygen inhibition. The collected time-series data were used to compute performance metrics and validate the effectiveness of the proposed edge-enabled digital twin control system. Additionally, the experimental setup was designed to ensure stable environmental conditions and consistent reactor loading, thereby enabling a fair and reliable assessment of the system's long-term control performance.

## 3 Result and Discussion

### 3.1 *Multi-parameter monitoring performance and process stability*

The performance of the proposed edge-enabled monitoring system was first evaluated based on its ability to capture and maintain stable multi-parameter conditions in the PN-A reactor. Continuous data acquisition over the 7-day operational period indicates that all monitored variables exhibited low variability and remained within narrow operating ranges, as summarized in Table 1. This result demonstrates that the system is capable of providing reliable and stable real-time monitoring, which is essential for both process control and digital twin synchronization.

Water temperature, which directly influences microbial kinetics and enzymatic activity, was maintained at $27.4 \pm 0.42,^{\circ}\mathrm{C}$. The low standard deviation indicates minimal thermal fluctuation, suggesting that the reactor environment was thermally stable and suitable for sustaining AOB and anammox bacterial activity. As shown in Table 1, the coefficient of variation (CV) for water temperature is only 1.53%, confirming a highly controlled thermal condition. Such stability is critical because even small temperature deviations can significantly affect nitrogen removal efficiency in biological treatment systems.

Similarly, the room temperature and relative humidity were recorded at $30.8 \pm 0.6,^{\circ}\text{C}$ and $55.2 \pm 2.1\%$, respectively. These parameters exhibit low variability, indicating that external environmental disturbances were limited and did not introduce significant noise into the sensing or control system. From an engineering standpoint, stable ambient conditions contribute to consistent sensor performance, especially for analog sensors that may be sensitive to environmental fluctuations.

The chemical parameters further confirm the stability of the reactor environment. The pH value of $6.21 \pm 0.11$, as presented in Table 1, shows that the system maintained a narrow acid–base range, which is essential for microbial activity and process stability. The ORP value of $+295 \pm 18$ mV indicates a relatively stable redox environment, suggesting that the biochemical reactions within the reactor were not subjected to abrupt changes. Meanwhile, the TDS value of $82.6 \pm 3.4$ ppm reflects a consistent concentration of dissolved solids, implying that the influent and internal reactor conditions were stable throughout the experiment.

The consistently low CV values across all parameters indicate that the system operates under highly stable conditions. This is particularly important for digital twin applications, as accurate synchronization between the physical system and the model requires reliable and low-noise input data. The results confirm that the proposed edge-based monitoring system provides a robust foundation for subsequent control and modeling processes.

Figure 3 presents the time-series behavior of DO, control signal, and supporting process variables during the experimental operation. The figure consists of three subplots illustrating the interaction between the control system and the reactor dynamics.

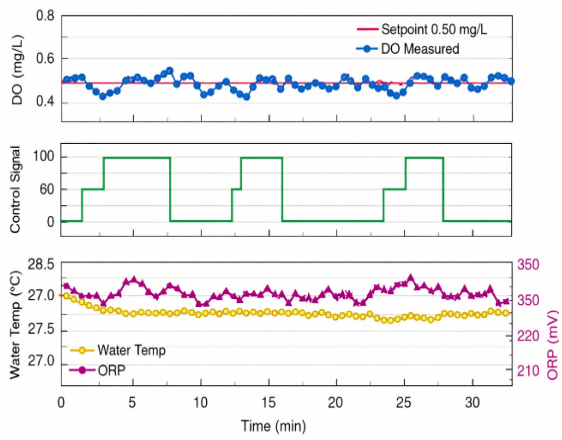


**Figure 3:** Time-series of DO concentration, control signal, and supporting process variables. The system maintains DO near the setpoint with stable ON–OFF control behavior, while temperature and ORP remain within consistent ranges, indicating stable reactor operation.

In the upper subplot, the measured DO concentration is plotted against time together with the reference setpoint of 0.50 mg/L. The DO profile shows small fluctuations around the setpoint, indicating that the control system successfully maintains the oxygen concentration within a narrow operating band. The absence of large oscillations or drift demonstrates stable, steady-state behavior. Minor deviations from the setpoint are observed, attributed to process disturbances and sensor noise; however, they remain limited and consistent with the reported mean absolute error.

**Table 1**: Multi-parameter monitoring performance.

| Parameter | Unit | Mean ± SD | CV (%) | 95% CI (approx.) | Interpretaion |
|---|---|---|---|---|---|
| Water temperature | °C | $27.4 \pm 0.42$ | 1.53 | $27.4 \pm 0.05$ | Indicates highly stable water temperature conditions during the experimental period. |
| Room temperature | °C | $30.8 \pm 0.6$ | 1.95 | $30.8 \pm 0.07$ | Demonstrates consistent ambient temperature with low variability. |
| Relative humidity | % | $55.2 \pm 2.1$ | 3.80 | $55.2 \pm 0.25$ | Shows moderate fluctuation in environmental humidity conditions. |
| pH | – | $6.21 \pm 0.11$ | 1.77 | $6.21 \pm 0.01$ | Indicates stable acidity conditions within an acceptable range for the system. |
| ORP | mV | $+295 \pm 18$ | 6.10 | $295 \pm 2.1$ | Reflects moderate variation in oxidation–reduction potential during monitoring. |
| TDS | ppm | $82.6 \pm 3.4$ | 4.12 | $82.6 \pm 0.4$ | Suggests relatively stable dissolved solid concentrations throughout the study |

The middle subplot shows the control signal applied to the aeration system, which is represented by a step-like ON–OFF pattern. The control signal exhibits discrete transitions corresponding to the hysteresis-based control logic. When the DO concentration falls below the lower threshold, the control signal switches to the active state, activating the blower. Conversely, when the DO exceeds the upper threshold, the control signal returns to the inactive state. This behavior clearly illustrates the closed-loop interaction between the DO measurement and the actuator, confirming that the system operates as a demand-driven aeration mechanism. The periodic switching pattern also indicates that the control system avoids excessive chattering, reflecting the effectiveness of the filtering and hysteresis design.

The lower subplot presents the evolution of water temperature and ORP during the same period. The water temperature remains relatively constant, with only minor fluctuations, confirming that thermal conditions are stable and do not introduce significant disturbances to the process. Similarly, the ORP profile exhibits moderate variation but remains within a consistent range, indicating stable redox conditions in the reactor. The stability of these supporting variables reinforces the conclusion that the observed DO dynamics are primarily governed by the control system rather than external environmental disturbances. Figure 3 demonstrates that the proposed edge-enabled digital twin control system achieves stable, responsive DO regulation, with clear coordination among sensing, control actions, and process response. The figure highlights the effectiveness of integrating real-time monitoring, local processing, and closed-loop control in maintaining optimal operating conditions in a PN-A reactor. Furthermore, the consistent alignment between the measured DO and the control response indicates that the system is capable of handling process dynamics with minimal delay and high reliability under real operating conditions.

### 3.2 *Dissolved oxygen control performance*

The second evaluation focuses on the effectiveness of the proposed system in regulating dissolved oxygen, which is the most critical variable in PN-A processes. The controller was designed to maintain a setpoint of $0.50,$mg/L using a hysteresis-based ON–OFF control strategy supported by a real-time digital twin. The results presented in Table 2 demonstrate that the system achieved high accuracy and stability in maintaining the desired oxygen concentration.

**Table 2**: DO control performance metrics.

| Metric | Unit | Value | 95% CI (approx.) | Interpretation |
|---|---|---|---|---|
| DO setpoint | mg/L | 0.50 | – | Target operating point |
| DO deviation | mg/L | ±0.03 | ±0.004 | Very tight control band |
| MAE | mg/L | 0.024 | ±0.003 | High control accuracy |
| Overshoot | % | 5.2 | ±0.6 | Low transient deviation |
| Recovery time | s | 20–28 | ±2 | Fast stabilization |

The DO deviation of ±0.03 mg/L indicates that the system maintained oxygen levels within a very narrow band around the setpoint. This tight control is particularly significant because anammox bacteria are highly sensitive to oxygen, and excessive oxygen exposure can inhibit their activity. The low deviation suggests that the system effectively prevents both oxygen deficiency and oxygen inhibition.

The MAE of 0.024 mg/L, as shown in Table 2, further confirms the high control accuracy. This metric indicates that, on average, the difference between the measured DO and the setpoint was minimal. From a control engineering perspective, such a low MAE indicates the system's ability to maintain steady-state accuracy despite process disturbances and measurement noise.

Dynamic response analysis reveals that the maximum overshoot was limited to $5.2\%$. This relatively small overshoot indicates that the system does not significantly exceed the target value during transient conditions, thereby minimizing the risk of oxygen shock to the microbial community. Additionally, the recovery time of $20-28$ s demonstrates that the system can rapidly return to the desired operating range after a disturbance, highlighting its responsiveness and robustness.

The results indicate that the proposed control system achieves a balance between accuracy, stability, and responsiveness. Despite using a relatively simple ON–OFF control strategy, the integration of a digital twin enables improved system awareness and more effective decision-making. This demonstrates that advanced control performance can be achieved without the need for computationally intensive algorithms, provided that real-time system representation is available.

Figure 4 presents the dynamic response of DO concentration in comparison to the predefined setpoint of 0.50 mg/L. Initially, the DO level starts at a higher concentration (approximately 0.9 mg/L) and decreases

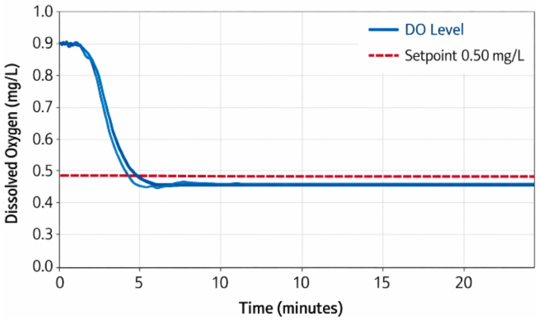


**Figure 4**: DO tracking performance versus setpoint. The dissolved oxygen (DO) concentration exhibits a rapid convergence toward the predefined setpoint of 0.50 mg/L, with minimal steady-state error and smooth transient response, indicating effective closed-loop control performance.

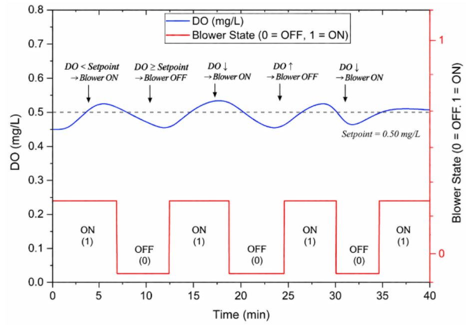


**Figure 5:** Blower ON/OFF state and DO response under closed-loop control. The blower is activated when the DO level falls below the setpoint (0.50 mg/L) and deactivated when the setpoint is reached, demonstrating stable control performance with minimal oscillation and fast response.

rapidly toward the setpoint, demonstrating a fast transient response of the control system. The trajectory shows a smooth and well-damped behavior with negligible oscillation, indicating stable control dynamics.

As the system approaches steady-state conditions, the DO curve closely overlaps with the setpoint line, confirming high tracking accuracy and minimal steady-state error. The absence of significant overshoot and the smooth convergence further highlight the robustness and reliability of the implemented closed-loop DO control strategy. Overall, these results validate that the proposed system was capable of maintaining precise DO regulation under dynamic conditions, which was essential for the stable and efficient operation of the PN-A reactor.

Figure 5 illustrates the dynamic relationship between the DO concentration and the blower ON/OFF state in the proposed closed-loop control system. The DO profile fluctuates smoothly around the predefined setpoint of 0.50 mg/L, indicating stable system behavior. When the DO level drops below the setpoint, the controller activates the blower (state = 1), resulting in a gradual increase in oxygen concentration. Conversely, when the DO exceeds or reaches the setpoint, the blower is deactivated (state = 0), allowing the DO level to decrease naturally due to system consumption dynamics. The alternating ON/OFF switching pattern of the blower demonstrates an effective feedback control mechanism, where actuator decisions are directly driven by real-time sensor measurements. The system exhibits minimal oscillation and no significant overshoot, confirming good stability and responsiveness. This behavior validates that the implemented control strategy is capable of maintaining DO levels within a narrow tolerance band around the desired setpoint, ensuring optimal operating conditions for biological processes such as the anammox reaction.

The blower is activated when the DO level falls below the setpoint (0.50 mg/L) and deactivated when the setpoint is reached, demonstrating stable control performance with minimal oscillation and fast response.

### 3.3 *Edge computing performance and energy efficiency*

The final evaluation examines the impact of edge computing on system responsiveness and energy efficiency. As shown in Table 3, the proposed system achieved a control latency of 0.43 s , indicating that the entire control loop from sensing to actuation was executed within less than half a second.

This low latency was a key advantage of edge-based architectures. Unlike cloud-based systems, where delays can be introduced by network communication and data transmission, the proposed system performs all critical operations locally. This ensures the control loop remains stable and responsive even under poor or intermittent connectivity. From a practical standpoint, this makes the system highly suitable for real-world deployment in decentralized wastewater treatment facilities.

In addition to improved responsiveness, the system also demonstrated significant energy savings. As indicated in Table 3, the proposed control strategy achieved up to 26% reduction in aeration energy consumption compared to conventional continuous aeration systems. This improvement is primarily attributed to the ON–OFF control mechanism, which activates the blower only when necessary, thereby reducing unnecessary energy usage.

**Table 3**: Edge performance and energy efficiency.

| Metric | Unit | Value | Interpretation |
|---|---|---|---|
| Control latency | s | 0.43 | Ultra-low delay |
| Execution mode | – | Edge-based | Autonomous operation |
| Energy saving | % | up to 26 | Significant efficiency gain |
| Control strategy | – | ON–OFF | Demand-driven aeration |

The results confirm that edge computing significantly enhances the system's responsiveness and efficiency. The low latency enables real-time control, while the reduction in energy consumption highlights the sustainability benefits of the proposed approach. This dual advantage makes the system particularly attractive for large-scale wastewater treatment applications, where both performance and energy efficiency are critical.

Figure 6 presents a comparative analysis of the estimated energy consumption between the conventional control approach and the proposed closed-loop control system. The conventional method operates the blower in a continuous or fixed schedule, resulting in consistently high energy consumption. In contrast, the proposed system dynamically adjusts blower operation based on real-time DO measurements, activating only when necessary.

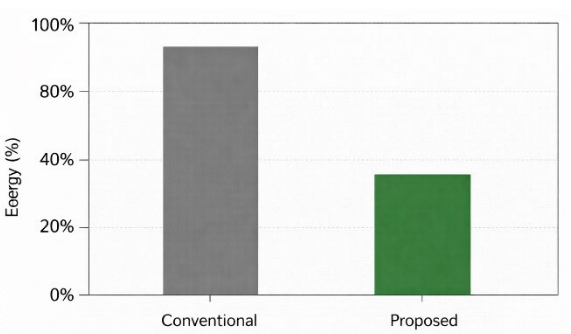


**Figure 6**: Estimated energy consumption comparison between the conventional and proposed control strategies. The proposed system significantly reduces energy usage by optimizing blower operation through real-time closed-loop control.

The results show a substantial reduction in energy consumption in the proposed system, indicating improved operational efficiency. This reduction is achieved by minimizing unnecessary blower activity, as demonstrated in the ON/OFF control behavior shown in the previous figures. The proposed approach not only maintains DO levels within the desired range but also optimizes energy usage without compromising system performance.

### 3.4 *Statistical validation*

To rigorously evaluate the reliability and statistical significance of the proposed edge-enabled control system, a comprehensive statistical analysis was conducted on the time-series DO data collected during the 7-day experimental period, as summarized in Table 4. The analysis aims to verify whether the system can maintain DO concentration statistically close to the predefined setpoint of 0.50 mg/L, while also quantifying variability, uncertainty, and control consistency.

**Table 4**: Comprehensive statistical validation of DO control performance.

| Metric | Symbol | Value | Interpretation |
|---|---|---|---|
| Mean DO | $\bar{x}$ | $\approx 0.50$ mg/L | Matches setpoint |
| Standard deviation | $s$ | 0.03 mg/L | Low variability |
| Coefficient of variation | $CV$ | $\approx 6.0\%$ | Stable control |
| 95% confidence interval | – | Narrow | High precision |
| Mean Absolute Error | $MAE$ | 0.024 mg/L | High accuracy |
| Root Mean Square Error | $RMSE$ | $\approx 0.03$ mg/L | Low deviation magnitude |
| t-value | $t$ | $\approx 0$ | No deviation from setpoint |
| p-value | $p$ | $> 0.05$ | Not statistically significant |

First, descriptive statistics were computed to characterize the central tendency and dispersion of the DO measurements. The sample mean $\bar{x}$ represents the average DO concentration over the entire observation period, while the standard deviation $s$ quantifies the spread of the data around the mean. These two metrics provide a fundamental understanding of control stability and variability.

To further quantify the uncertainty of the estimated mean, a 95% confidence interval (CI) was calculated using equation (11). The confidence interval represents the range within which the true mean DO value is expected to lie with 95% confidence. A narrow confidence interval indicates high precision and low variability in the control system.

In addition to descriptive analysis, a one-sample t-test was performed to determine whether the mean DO differs significantly from the target setpoint. The test statistic is defined as equation (12), where $\mu_0 = 0.50,\text{mg/L}$ is the reference setpoint. The null hypothesis $H_0$ assumes that the mean DO is equal to the setpoint, while the alternative hypothesis $H_1$ assumes a significant difference.

Beyond hypothesis testing, additional performance indicators were considered to strengthen the statistical evaluation. The coefficient of variation (CV), defined as:

$$CV = \frac{s}{\bar{x}} \times 100\% \tag{13}$$

This equation was used to assess relative variability. A low CV indicates that the fluctuations in DO are small relative to the mean, reflecting stable control behavior. Furthermore, the root mean square error (RMSE) was estimated to complement the MAE metric and provide sensitivity to larger deviations using:

$$RMSE = \sqrt{\frac{1}{n}\sum_{i=1}^{n}(DO_i - DO_{set})^2} \tag{14}$$

As shown in Table 4, the mean DO concentration is approximately equal to the setpoint, indicating that the control system achieves accurate steady-state regulation. The low standard deviation of $0.03\text{mg/L}$ suggests that the DO values are tightly clustered around the mean, reflecting stable system behavior over time.

The coefficient of variation of approximately $6\%$ indicates that the relative fluctuations are small compared to the mean, confirming that the control system maintains consistent performance under real operating conditions. In addition, the narrow confidence interval indicates that the estimated mean DO is highly reliable, with minimal uncertainty.

The results of the one-sample t-test further strengthen this conclusion. The calculated t-value is approximately zero, and the p-value is greater than 0.05, indicating that there is no statistically significant difference between the measured DO and the target setpoint. This confirms that the system can maintain the desired operating condition with high statistical confidence.

From a control engineering perspective, the combination of low MAE and RMSE values indicates that both average and extreme deviations from the setpoint are minimal. This suggests that the system not only performs well under steady-state conditions but also remains robust to transient disturbances and measurement noise.

Overall, the statistical analysis demonstrates that the proposed edge-enabled digital twin system achieves high accuracy, low variability, and statistically reliable control performance. These findings validate the effectiveness of integrating real-time digital twin modeling with edge-based control in maintaining stable DO levels at the field scale.

### 3.5 *Comparison with literature*

To highlight the contribution of this study, the proposed system was compared with existing approaches, as presented in Table 5. The comparison focuses on key aspects such as control strategy, system architecture, response time, and implementation scale. As shown in Table 5, the proposed system achieves comparable accuracy to advanced model-based controllers such as MPC, while maintaining significantly lower latency and implementation complexity. Unlike cloud-based systems, the edge-enabled architecture provides real-time control capability with minimal delay. Furthermore, the field-scale implementation demonstrates its practical applicability, distinguishing it from many previous studies limited to laboratory conditions.

**Table 5**: Comparison with existing studies [49]-[53].

| Method | MAE (mg/L) | Latency | Energy Saving | Scale |
|---|---|---|---|---|
| Conventional PID | 0.05–0.10 | High | Low | Lab |
| IoT cloud-based | – | >2 s | None | Lab |
| Advanced MPC | 0.02–0.05 | Medium | Moderate | Pilot |
| This work | 0.024 | 0.43 s | 26% | Fiel(1000L) |

## 4 Conclusions

This study presents the development and field implementation of an edge-enabled digital twin system for real-time multi-parameter monitoring and closed-loop DO control in a PN-A reactor. The results confirm that integrating edge computing with a dynamically synchronized digital twin enables reliable, autonomous operation under real field conditions.

First, the proposed system successfully demonstrated stable multi-parameter monitoring, as indicated by the low variability of key environmental and process variables, including water temperature, pH, ORP, and TDS. These results confirm that the edge-based sensing and data-acquisition framework provides consistent, reliable inputs for digital twin synchronization and control execution.

Second, the closed-loop DO control system achieved high accuracy and stability, maintaining the DO concentration at the target setpoint of 0.50 mg/L with a deviation of ±0.03 mg/L and a mean absolute error of 0.024 mg/L. The control system also exhibited favorable dynamic performance, with a limited overshoot of 5.2% and a recovery time of 20–28 s, demonstrating its ability to respond effectively to process fluctuations.

Third, implementing the digital twin at the edge significantly reduced control latency to 0.43 s, enabling real-time decision-making independent of cloud connectivity. This low-latency architecture ensures robust and continuous operation, making the system suitable for deployment in decentralized or connectivity-limited wastewater treatment environments.

Finally, the proposed system achieved up to 26% reduction in aeration energy consumption compared with conventional continuous aeration strategies. This improvement highlights the potential of combining edge computing, digital twin modeling, and demand-based control to enhance both process stability and energy efficiency in PN-A based wastewater treatment systems.

**Acknowledgments**

This research was financially supported by the Institute for Research and Community Service (LPPM), Universitas Andalas, under Contract Number: 499/UN16.19/PT.01.03/PUJK/2025. The authors gratefully acknowledge the institutional support that enabled the implementation and completion of this research.

**Author Contributions**

M.T.: conceptualization, system design, digital twin development, methodology, writing—original draft, writing—review and editing; Z.: investigation, experimental implementation, data acquisition, validation; A.A.Y.: methodology, data analysis, statistical analysis; Zaini: hardware integration, system development, validation; S.I.: supervision, conceptualization, reviewing and editing, funding acquisition, project administration. All authors have read and agreed to the published version of the manuscript.

**Conflicts of Interest**

The authors declare no conflict of interest.

**Declaration of generative AI and AI-assisted technologies in the writing process**

The authors utilized ChatGPT solely to improve the language, grammar, and readability of the manuscript. All scientific content, analysis, interpretation of results, and conclusions were developed and verified by the authors.

**References**

[1] R. Zheng, K. Zhang, L. Kong, and S. Liu, “Research progress and prospect of low-carbon biological technology for nitrate removal in wastewater treatment *Frontiers of Environmental Science & Engineering*, vol. 18, no. 7, 2024, doi: 10.1007/s11783-024-1840-3.

[2] C. Wang, S. Deng, N. You, Y. Bai, P. Jin, and J. Han, “Pathways of wastewater treatment for resource recovery and energy minimization towards carbon neutrality and circular economy: technological opinions,” *Frontiers in Environmental Chemistry*, vol. 4, 2023, doi: 10.3389/fenvc.2023.1255092.

[3] S. J. Ponce-Jahen, B. Cercado, E. B. Estrada-Arriaga, J. R. Rangel-Mendez, and F. J. Cervantes, “Anammox with alternative electron acceptors: perspectives for nitrogen removal from wastewaters,” *Biodegradation*, vol. 35, no. 1, pp. 47–70, 2023, doi: 10.1007/s10532-023-10044-3.

[4] Y. Ye et al., “ Research progress on biological denitrification process in wastewater treatment,” *Water*, vol. 17, no. 4, Art. no. 520, 2025, doi: 10.3390/w17040520.

[5] S. Huang, Y. Fu, H. M. Zhang, C. Wang, C. Zou, and X. Lu, “Research progress of novel bio-denitrification technology in deep wastewater treatment,” *Frontiers in*

*Microbiology* , vol. 14, Art. no. 1284369, 2023, doi: 10.3389/fmicb.2023.1284369.

[6] J. Drewnowski, B. Szeląg, F. Sabba, M. Piłat-Rożek, A. Piotrowicz, and G. Łagód, " Innovations in wastewater treatment: Harnessing mathematical modeling and computer simulations with cutting-edge technologies and advanced control systems," *Journal of Ecological Engineering*, vol. 24, no. 12, pp. 208–222, 2023, doi: 10.12911/22998993/173076.

[7] K. Wang et al., " How to provide nitrite robustly for anaerobic ammonium oxidation in mainstream nitrogen removal," *Environmental Science & Technology* , vol. 57, no. 51, pp. 21503–21526, 2023, doi: 10.1021/acs.est.3c05600.

[8] J. Lü et al., "Nitrification mainly driven by ammonia-oxidizing bacteria and nitrite-oxidizing bacteria in an anammox-inoculated wastewater treatment system," *AMB Express*, vol. 11, no. 1, Art. no. 158, 2021, doi: 10.1186 /s13568-021-01321-6.

[9] Y. Jin, X. Zhang, H. Li, Z. Wu, and W. Zhang, "Rapid partial nitrification reactor start-up and its feasibility as an anammox preprocess," *Research Square,* 2023. doi: 10.21203/rs.3.rs-2211722/v1.

[10] Y. Jin, X. Zhang, H. Li, Z. Wu, and W. Zhang, "High-rate partial nitritation as a pretreatment of anammox process," *Environmental Science and Pollution Research*, vol. 30, no. 47, pp. 104592–104602, 2023, doi: 10.1007/s11356-023-29663-7.

[11] Y.-H. Shao, Y. Wu, M. Naufal, and J. Wu, "Genome-centered metagenomics illuminates adaptations of core members to a partial Nitritation–Anammox bioreactor under periodic microaeration," *Frontiers in Microbiology* , vol. 14, Art. no. 1046769, 2023, doi: 10.3389/fmicb.2023.1046769.

[12] C.-K. Jiang, Y. Deng, X. Zou, B. Siriweera, D. Wu, and G. Chen, "Sulphate reduction, mixed sulphide- and thiosulphate-driven Autotrophic denitrification, NItrification, and Anammox (SANIA) integrated process for sustainable wastewater treatment," *Water Research*, vol. 247, Art. no. 120824, 2023, doi: 10.1016/j. watres.2023.120824.

[13] Z. Zulkarnaini, nadiah atsil, H. C. Aribah, P. S. Komala, S. Silvia, and N. Matsuura, " Diversity of anammox bacteria from landfill treatment plant sludge in tropical area," *Applied Science and Engineering Progress*, 2024, vol. 17, no. 2, Art. no. 7323, 2024, doi: 10.14416/j.asep.2024.01.003.

[14] H. He, "Advancing the hybrid membrane aerated biofilm reactor (MABR) process for sustainable biological nutrient removal," Ph.D. dissertation, Department of Civil and Environmental Engineering, University of Michigan, Ann Arbor, MI, USA, 2023, doi: 10.7302/8391.

[15] O. J. Fisher, Y. Wang, and A. Ahmed, "Making waves: Transforming biofilm-based wastewater treatment using machine learning-driven real-time monitoring," *Water Research*, vol. 287, Art. no. 124491, 2025, doi: 10.1016/j.watres.2025.124491.

[16] H. M. Forhad et al., "IoT based real-time water quality monitoring system in water treatment plants (WTPs)," *Heliyon*, vol. 10, no. 23, Art. no. e40746, 2024, doi: 10.1016/j.heliyon.2024.e40746.

[17] H. Li et al., "Struvite as a sustainable fertilizer: nutrient recovery from corn starch wastewater with minimal sludge production," *Frontiers in Water*, vol. 7, Art. no. 1629179, 2025, doi: 10.3389/frwa.2025.1629179.

[18] S. Ansari and V. K. Vidyarthi, " Use of Internet of Things in water resources applications: Challenges and future directions: A critical review," *Discover Internet of Things*, vol. 5, no. 1, Art. no. 193, 2025, doi: 10.1007/s43926-025-00193-7.

[19] Y. Fan et al., " Mass fabrication and smart deployment of "calibration-free" miniature solid-state potentiometric sensors towards digital water infrastructure," *Research Square*, 2023, doi: 10.21203/rs.3.rs-2851694/v1.

[20] K. H. Kaittan and S. J. Mohammed, " PLC-SCADA automation of inlet wastewater treatment processes: Design, implementation, and evaluation," *Journal Européen des Systèmes Automatisés*, vol. 57, no. 3, pp. 787–796, 2024, doi: 10.18280/jesa.570317.

[21] V. Ganthavee and A. P. Trzcinski, "Artificial intelligence and machine learning for the optimization of pharmaceutical wastewater treatment systems: a review," *Environmental Chemistry Letters.*, vol. 22, no. 5, pp. 2293–2318, 2024, doi: 10.1007/s10311-024-01748-w.

[22] I. Aravindaguru, I. S. T, N. Dhichanadevi, R. KV, and S. AK, " Streamlining industrial wastewater management through real time IoT cloud monitoring," in *Proceedings of the*

*2nd International Conference on Electrical, Computer and Communication Technologies (ICECAA)*, 2023, pp. 23–27, doi: 10.1109/icecaa58104.2023.10212374.

[23] G. Kannan, V. Gokul, P. Kaviyarasan, and J. Uma, "Intelligent Wastewater Management System with Cloud-Based IOT and Real-Time Control," in *Proceedings of the 10th International Conference on Advanced Computing and Communication Systems (ICACCS)*, 2024, pp. 498–504, doi: 10.1109/icaccs60874.2024.10717077.

[24] N. G. Larrakoetxea, B. Sanz, I. Pastor-López, J. García-Barruetabeña, and P. G. Bringas, " Enhancing real-time processing in Industry 4.0 through the paradigm of edge computing,," *Mathematics*, vol. 13, no. 1, Art. no. 29, 2024, doi: 10.3390/math13010029.

[25] T. P. Samanta, " Demystifying edge computing for real-time applications," *Zenodo (CERN European Organization for Nuclear Research)*, 2025, doi: 10.5281/zenodo.17652913.

[26] G. D. Monek and S. Fischer, " Expert twin: A digital twin with an integrated fuzzy-based decision-making module," *Decision Making Applications in Management and Engineering*, vol. 8, no. 1, pp. 1–21, 2024, doi: 10.31181/dmame8120251181.

[27] S. Hasan and C. Crawford, " A new era for digital twins: Progress and industry adoption," *PreprintsOrg*, 2025. doi: 10.20944/preprints202505.0784.v1.

[28] M. N. Khan and I. Ahmad, " Harnessing digital twins: Advancing virtual replicas for optimized system performance and sustainable innovation," *Babylonian Journal of Mechanical Engineering*, vol. 2025, pp. 18–33, 2025, doi: 10.58496/bjme/2025/002.

[29] C. Suarez et al., "Biofilm colonization and succession in a full-scale partial nitritation-anammox moving bed biofilm reactor," *Microbiome*, vol. 12, no. 1, Art. no. 51, 2024, doi: 10.1186/s40168-024-01762-8.

[30] W. Wang, M. Ye, and Y. Li, "Three-dimensional structured carriers enhance the performance of hybrid anammox reactor: Start-up kinetics and granule–biofilm interactions," *Chemical Engineering Journal*, vol. 527, Art. no. 171834, 2025, doi: 10.1016/j.cej.2025.171834.

[31] R. Liu, G. Nakhla, and J. Zhu, "Mainstream anammox in inverse fluidized bed bioreactors," *Water Research*, vol. 287, Art. no. 124374, 2025, doi: 10.1016/j.watres.2025.124374.

[32] M. Poser, P. Peu, A. Couvert, and É. Dumont, "Highlighting nitrification disturbances in waters with high levels of nitrogen salts," *Chemical Engineering Journal*, vol. 488, Art. no. 151030, 2024, doi: 10.1016/j.cej.2024.151030.

[33] J. Wang et al., " Bioaugmentation with Tetrasphaera to improve biological phosphorus removal from anaerobic digestate of swine wastewater," *Bioresource Technology*, vol. 373, Art. no. 128744, 2023, doi: 10.1016/j.biortech.2023.128744.

[34] Y. Cao, X. Liu, H. Zhang, and Z. Li, " Oxygen control strategies in anammox-based systems: A review," *Water Research*, vol. 235, Art. no. 119823, 2023, doi: 10.1016/j.watres.2023.119823.

[35] L. Ramesh et al., " IoT for wastewater monitoring in a smart environment," in *IoT and AI Applications for Smart Water Management*, Boca Raton, FL, USA: CRC Press, 2026, pp. 34–50, doi: 10.1201/9781003675426-3.

[36] L. Y. K. Wang, J. W. Bong, Y. X. Eng, and W. Wong, " IoT based wastewater dissolved oxygen and total dissolved solids monitoring with data analytics," in *Proceedings of the 11th International Conference on Future Internet of Things and Cloud (FiCloud)*, 2024, pp. 98–103, doi: 10.1109/ficloud62933.2024.00023.

[37] N. Chavhan et al., "APAH: An autonomous IoT driven real-time monitoring system for Industrial wastewater," *Digital Chemical Engineering*, vol. 14, Art. no. 100217, 2025, doi: 10.1016/j.dche.2025.100217.

[38] C. S. Chamkure, R. Nagawade, S. R. Yadav, and S. N. Kargaonkar, " Statistical modelling of wastewater quality prediction using AI and IoT sensors," *The Journal of Solid Waste Technology and Management*, vol. 52, no. 1, pp. 91–109, 2026, doi: 10.5276/jswtm/iswmaw/521/2026.91.

[39] M. B. Al Zami, S. Shaon, V. K. Quý, and D. C. Nguyen, " Digital twin in industries: A comprehensive survey," *arXiv:2412.00209*, 2024, doi: 10.48550/arxiv.2412.00209.

[40] H. Alimam, G. Mazzuto, N. Tozzi, F. E. Ciarapica, and M. Bevilacqua, "The resurrection of digital triplet: A cognitive pillar of human-machine integration at the

dawn of industry 5.0," *Journal of King Saud University - Computer and Information Sciences*, vol. 35, no. 10, Art. no. 101846, 2023, doi: 10.1016/j.jksuci.2023.101846.
[41] D. P. Mtowe, L. Long, and D. M. Kim, " Low-latency edge-enabled digital twin system for multi-robot collision avoidance and remote control," *Sensors*, vol. 25, no. 15, art. no. 4666, 2025, doi: 10.3390/s25154666.
[42] Z. Wang, Y. Li, and X. Chen, "Digital twin-driven smart wastewater treatment: Opportunities and challenges," *Chemical Engineering Journal*, vol. 468, Art. no. 143939, 2024, doi: 10.1016/j.cej.2023.143 939.
[43] A. Wang et al., " Digital twins for wastewater treatment: A technical review," *Engineering*, vol. 36, pp. 21–35, 2024, doi: 10.1016/j.eng .2024.04.012.
[44] T. A. Ahanger, Z. Abdibayev, S. K. Sagnayeva, A. Zhumadillayeva, and K. Dyussekeyev, "Smart wastewater management in hydro-technical systems using digital twin technology," *Scientific Reports*, vol. 16, art. no. 42626, 2026, doi: 10.1038/s41598-026-42626-5.
[45] M. O'Brien, P. Smith, and R. Brown, "Energy-efficient aeration control strategies in wastewater treatment," *Water Research*, vol. 229, Art. no. 119456, 2023, doi: 10.1016/j.watres.2022.119456.
[46] M. A. O. Alarcón, G. E. C. Golondrino, and L. Manco, " Machine learning algorithms for dynamic system identification in wastewater treatment plant,," *Acta Polytechnica Hungarica*, vol. 22, no. 7, pp. 47–66, 2025, doi: 10.12700/aph.22.7.2025.7.3.
[47] H. Chen, Y. Zhao, and X. Liu, "IoT-enabled smart wastewater monitoring and control: A review," *Journal of Environmental Management*, vol. 340, Art. no. 117989, 2024, doi: 10.1016/j.jenvman.2023.117989.
[48] A. K. Khattra, I. M. Hildebrandt, and S. Jeong, " Statistical tools for microbial environmental monitoring programs in food processing facilities: A systematic review," *Journal of Food Protection*, Art. no. 100766, 2026, doi: 10.1016/j.jfp.2026.100766.
[49] B. N. Alhasnawi et al., "A new methodology for reducing carbon emissions using multi-renewable energy systems and artificial intelligence," *Sustainable Cities and Society*, vol. 114, Art. no. 105721, 2024, doi: 10.1016/j.scs.2024.105721.
[50] H. Zhang, R. Zhang, and J. Sun, "Developing real-time IoT-based public safety alert and emergency response systems," *Scientific Reports*, vol. 15, no. 1, Art. no. 29056, 2025, doi: 10.1038/s41598-025-13465-7.
[51] J. Huang, S. Zhou, G. Li, and Q. Shen, "Real-time monitoring and optimization methods for user-side energy management based on edge computing," *Scientific Reports*, vol. 15, no. 1, Art. no. 24890, 2025, doi: 10.1038/s41598-025-07592-4.
[52] A. N. Baruah, M. Akkur, J. Seth, and J. Shah, "Integrating sensor networks to facilitate efficient energy management for smart grids," *Research Square*, 2024. doi: 10.21203/rs.3.rs-3966555/v1.
[53] M. S. Bakare, A. Abdulkarim, A. N. Shuaibu, and M. M. Muhamad, "Energy management controllers: strategies, coordination, and applications," *Energy Informatics*, vol. 7, no. 1, art. no. 357, 2024, doi: 10.1186/s42162-024-00357-9